Recent advances in interior tomography (Mathematical Programming in the 21st Century : Algorithms and Modeling)

AUTHOR(S):

Rashed, Essam A.; Kudo, Hiroyuki

数理解析研究所講究録
第1676巻 2010年 145-156

Recent advances in interior tomography

Essam A. Rashed and Hiroyuki Kudo
Department of Computer Science, Graduate School of Systems and Information Engineering,
University of Tsukuba, Tennoudai 1-1-1, Tsukuba 305-8573, Japan
essam@imagelab.cs.tsukuba.ac.jp

Abstract

Computed Tomography (CT) is an imaging technique aims to observe the internal structure of an object using its projections. The projection data is generated using different modalities such as x-ray photon radiation in x-ray CT and positron radiation of a radioactive materials in Positron Emission Tomography (PET) and Single Photon Emission Computed Tomography (SPECT). The use of x-ray CT in medical imaging had been an essential tool for diagnosis and therapy in most of hospitals worldwide. In this paper, we consider a traditional problem in CT imaging known as the *interior tomography*. In this problem, measured projection data is truncated such that it is limited to the rays passing through a limited region located completely inside the object. We review the recent developments for this problem and present a new Bayesian approach for iterative reconstruction in interior tomography.

1 Introduction

In computed tomography (CT), the *interior tomography* (also called *local tomography*) is defined as the reconstruction of a region of interest (ROI) that is located completely inside the scanned object from limited projection data [1]. In this problem all projection rays are truncated such that left and right portions of the projection data are missing for all view angles. Two CT imaging configurations for full scan and ROI scan corresponding to the interior problem are shown in figure 1. It was believed for a long time that the solution of the interior problem is not unique even if the exact information on the object support (OS) is known [1]. The term object support refer to the contour line representing the object exact boundaries. As shown in figure 2 and the corresponding profiles in figure 3, when the projection data is truncated corresponding to the interior problem, the conventional Filtered Backprojection (FBP) reconstruction algorithm suffers from DC-shift and low-frequency artifacts. These artifacts may cause incorrect diagnosis in some clinical applications. Though the interior problem has been a topic in image reconstruction research for a long time (for example, see [2–6]), it is still a challenging problem. Recently, investigating

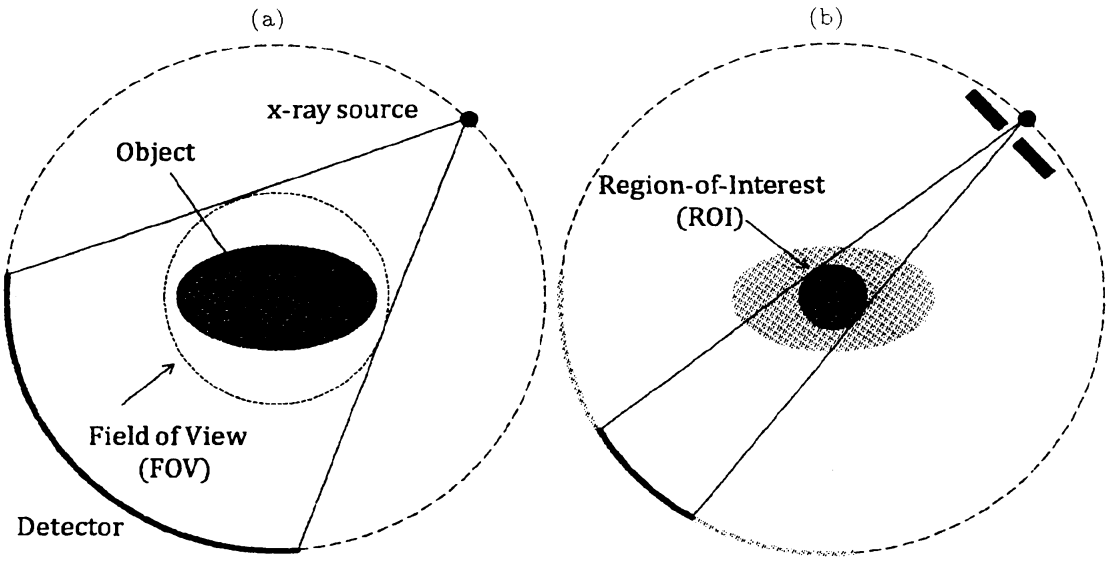

Figure 1: CT imaging configurations for (a) whole object imaging and (b) interior ROI imaging.

interior problem becomes a hot topic of research and new findings have been discovered. New discovery in interior problem has a several potential useful usage in clinical applications. For example, reducing the patient dose by focusing the radiation rays into a limited ROI in x-ray CT imaging, magnifying imaging without a requirement for hardware upgrade and suppressing scattering artifacts. In this paper, we overview the recent advances in finding the exact solution to the interior problem and present preliminary results obtained from the current research.

2 Recent Developments

2.1 Differentiated Backprojection (DBP)

Based on the concept of analytical reconstruction, it had been believed for a long time that ROI reconstruction, even for a small region, requires all projection rays passing through the whole object. However, the developed theories based on Differentiated Backprojection (DBP) [7] and Backprojection-Filtration (BPF) [8] succeeded in reducing the required set of projection rays for exact and stable ROI reconstruction. In these studies, an ROI can be reconstructed using the two-step Hilbert method if the ROI lies within the union of lines that do not contact the remaining portion of the object (i.e. ROI should includes both opposite boundaries of the object) as shown in figure 4(a). These results, obtained from analytical analysis, was also confirmed with a study based on iterative reconstruction using Maximum Likelihood Expectation-Maximization (ML-EM) algorithm in [9]. Later on, the sufficient conditions for accurate ROI

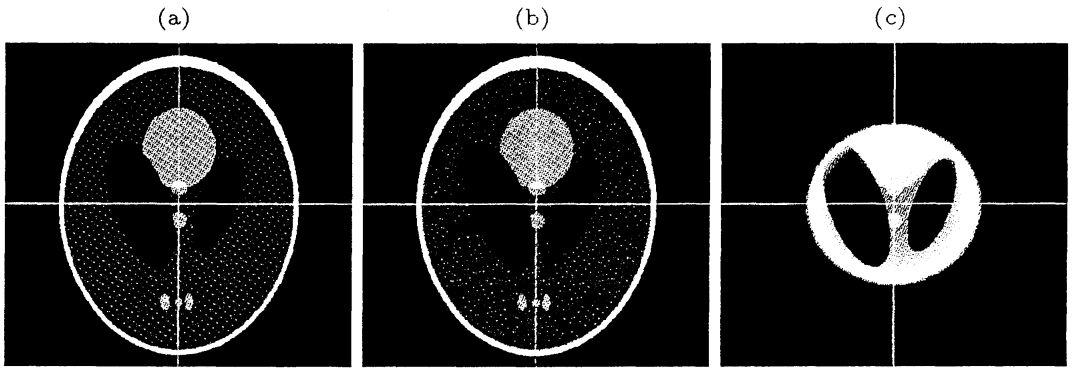

Figure 2: Reconstructed images of the Shepp-Logan phantom (high contrast). (a) The original phantom, the reconstructed images using FBP algorithm with (b) full scan and (c) interior ROI scan. Gray scale is [0.1 0.4].

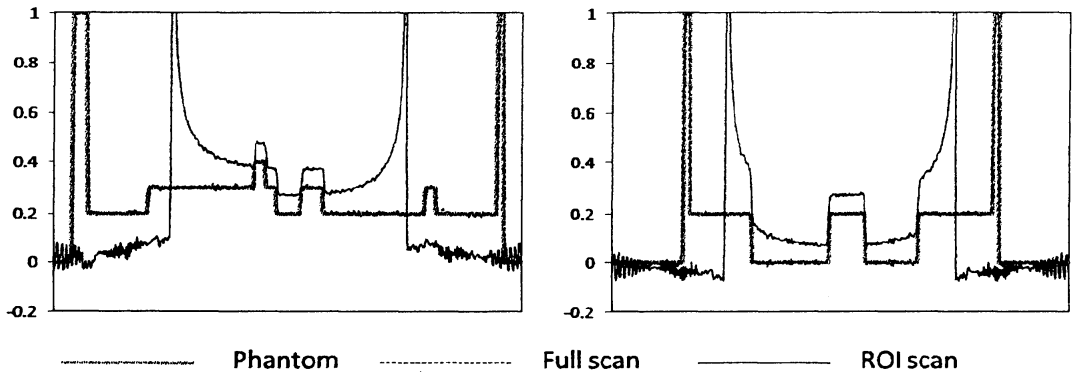

Figure 3: The vertical (left) and horizontal (right) profiles corresponding to the white line segments in figure 2.

reconstruction is relaxed in [10]. It is proved that the accurate reconstruction can be achieved by selecting the ROI such that it includes a single boundary of the object given that compact OS is well-defined (figure 4(b)). It became clear that the position of the ROI is an important factor to determine the possibility of accurate reconstruction.

As detailed in [10], by selecting the ROI such that it includes a limited region outside the compact OS (where the intensity values is *a priori* known to be zero), the accurate ROI reconstruction is possible. These results was extended to solve the interior problem by assuming that the *a priori* knowledge is available inside the ROI in [11–13]. This setup is shown in figure 4(c). Recently, the same approach was also reported to solve interior problem in SPECT imaging [14].

Since the analytical inversion formula for the imaging setups shown in figure 4(b) and (c) is not known yet, this theory was evaluated by using the DBP method with the projection onto convex sets (POCS) algorithm [10–13]. The same results can be obtain by using different iterative methods such as ML-EM

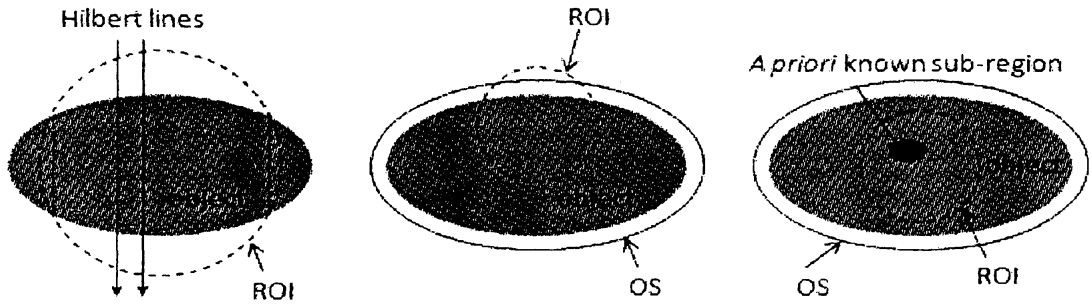

Figure 4: Definition of ROI for accurate reconstruction in the framework of DBP (a) Noo *et al.* 2004 and Pan *et al.* 2005, (b) Defrise *et al.* 2006 and (c) Kudo *et al.* 2008, Courdurier *et al.* 2008 and Ye *et al.* 2007.

reconstruction algorithm.

To illustrate the results achieved in [11–13] we apply a computer simulation using modified version of FORBILD thorax phantom. We select ROI as internal region covering the cardiac and assume that *a priori* knowledge corresponding to a small region located inside both the lung and ROI is available and OS is defined as the region corresponding to the 120% larger than the exact phantom. By using the ML-EM algorithm with 100 iterations, a significant improvement is recognized as shown in figure 5 and the corresponding profiles in figure 6.

2.2 Compressed Sensing (CS)

The theory of compressed sensing (also called *compressive sensing*) demonstrate that it is possible to reconstruct an accurate images from highly undersampled projection data [15, 16]. The main idea is to include a distance function consisting of ℓ_1/ℓ_0 norm of the reconstructed image into the cost function for image reconstruction. This technique based on the fact that ℓ_p norm ($0 \leq p \leq 1$) is effective in finding the sparse solution compared to the conventional ℓ_2 norm. The image sparsity is enforced by transforming the image into an appropriate domain such as discrete gradient or wavelet transforms. A recent study investigates solving the interior problem using the concept of compressed sensing is in [17]. It is stated that, the exact reconstruction of the interior ROI is possible by using Total Variation (TV) minimization assuming that the intensity values within each region (organ) is absolutely uniform.

2.3 Further extension

Recalling from the summery above, the exact reconstruction of interior ROI is hold if a compact OS of the object is defined and *a priori* information for a small sub-region is available. From practical point of view, the accurate *a priori* knowledge of internal structure is not easy to be achieved. In some limited clinical applications, the *a priori* information can be provided using known anatomical structure such as air in a trachea or dense bone. Also, the *a priori*

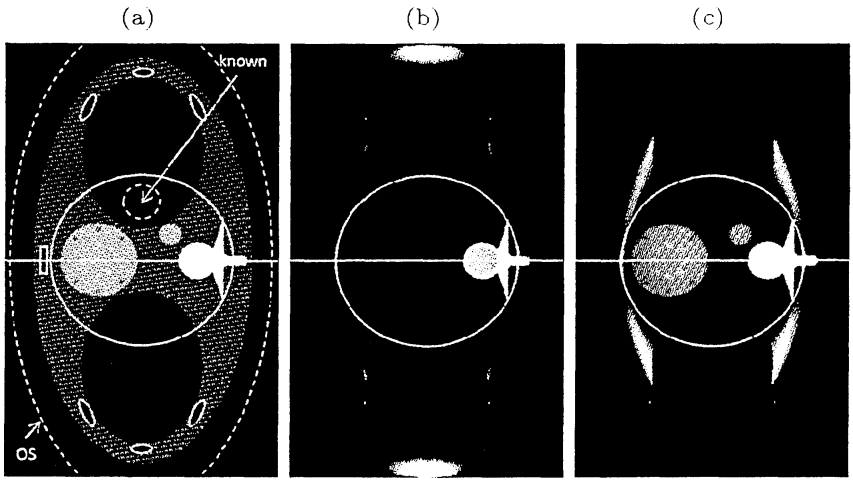

Figure 5: Reconstructed images of modified FORBILD thorax phantom. (a) Thorax phantom, object support, *a priori* known sub-region and interior ROI, reconstructed images by using ML-EM algorithm (b) without *a priori* knowledge and (c) with *a priori* knowledge corresponding to the small dashed circle in (a). Gray scale is [0.94 1.1].

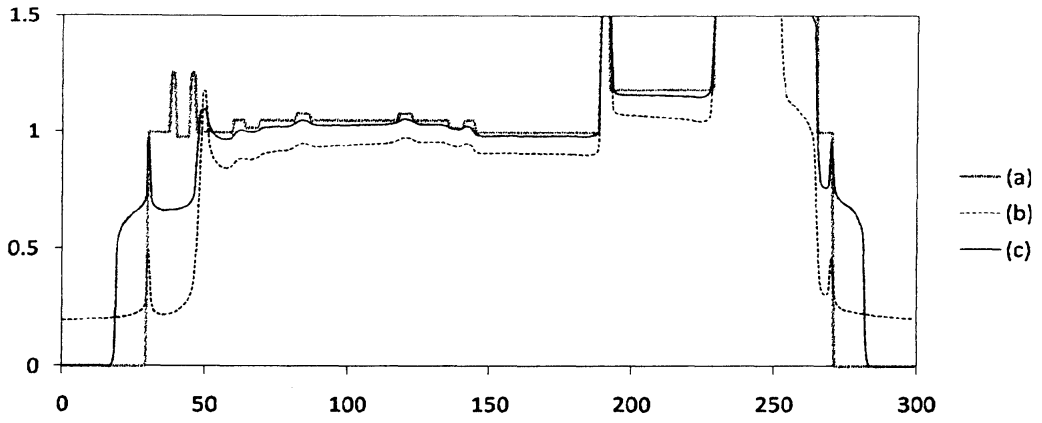

Figure 6: Profiles corresponding to the white line segments in figure 5.

information can be provided using a previous scan of the same patient. However, such techniques can lose their merits due to the registration errors. The point to be investigated here is, how to obtain an internal *a priori* information and at the same time avoid the registrations errors. In the following section, we will explain the details of the current research investigating this problem.

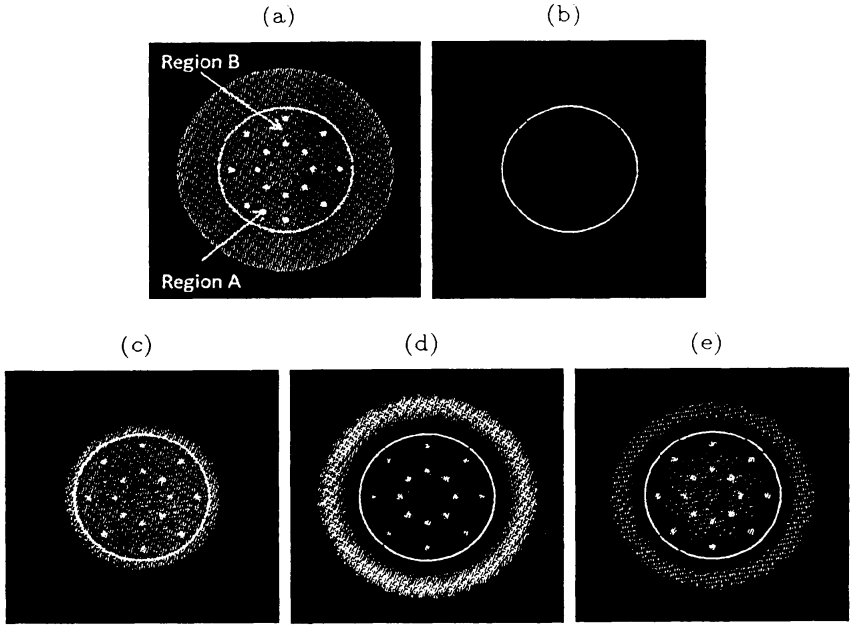

Figure 7: Reconstructed images of the disk phantom. (a) Phantom and interior ROI, reconstructed images with (b) OS-EM method, (c) R-MAP method with *a priori* knowledge corresponding region A, (d) R-MAP method with *a priori* knowledge corresponding region B, (e) same as (d) with 300 iterations. Gray scale is [0.9 1.1]

3 On going research

3.1 Bayesian framework for CT reconstruction

Recently, we have developed the R-MAP (Reference-MAP) and the I-MAP (Intensity-MAP) methods for image reconstruction from sparse projection data [18]. In these methods, the image reconstruction cost function includes two terms. The first term is the log-likelihood function and the second term is a distance function between the reconstructed image and a set of *a priori* known image/intensity values. In R-MAP method, the formulation of cost function is as follow

$$f_\beta(\vec{x}) = \underbrace{L(\vec{x})}_{\textit{negative log-likelihood function}} + \beta \underbrace{D(\vec{x}, \vec{x}^{ref})}_{\textit{distance function}} \tag{1}$$

$$L(\vec{x}) = \sum_{i=1}^{m} \left[\sum_{j=1}^{n} a_{ij} x_j - y_i \log \left(\sum_{j=1}^{n} a_{ij} x_j \right) \right] \tag{2}$$

$$D(\vec{x}, \vec{x}^{ref}) = \sum_{j=1}^{n} d(x_j, x_j^{ref}) \quad \text{and} \quad d(a,b) = |a-b| \tag{3}$$

where $\vec{x} = (x_1, \ldots, x_n)$ is the image vector, $\vec{y} = (y_1, \ldots, y_m)$ is the projection data, $A = \{a_{ij}\}$ is the $m \times n$ system matrix and $\vec{x}^{ref} = (x_1^{ref}, \ldots, x_n^{ref})$ is *a priori* known image (reference image) that contain regions expected in prior to imaging. The idea of R-MAP method was first disclosed in [19] to enhance PET/SPECT imaging using anatomical information extracted from MRI/CT scans. By using R-MAP method, we assume that the *a priori* information is available in the form of reference image. However, in I-MAP method, we relax this condition and the required *a priori* information is only a set of intensity values.

The implementation of the R-MAP and I-MAP methods is done by repeating the following two sub-steps. The first sub-step is the normal image update using the ML-EM algorithm. The second sub-step is a thresholding operations applied to the image obtained from the first sub-step. The thresholding function is designed such that it estimate the correct intensity values using the *a priori* information. The R-MAP method is summarized as follow

[STEP 1] (Preprocessing) Prepare the reference image $\vec{x}^{ref}$.
[STEP 2] (Initialization) Set the initial image as $\vec{x}^{(0)} = \vec{x}^{ref}$. Set the iteration number as $k \leftarrow 0$.
[STEP 3-1] (EM-update) Compute the image vector $\vec{p}$ by

$$p_j = \frac{x_j^{(k)}}{\sum_{i=1}^{m} a_{ij}} \sum_{i=1}^{m} \frac{a_{ij} y_i}{\sum_{j=1}^{n} a_{ij} x_j^{(k)}} \tag{4}$$

[STEP 3-2] (Intensity thresholding) Compute the image vector $\vec{q}$ by

$$q_j = \begin{cases} p_j - \delta_j & p_j > (x_j^{ref} + \delta_j) \\ p_j + \delta_j & p_j < (x_j^{ref} - \delta_j) \\ x_j^{ref} & (elsewhere) \end{cases}, \delta_j = \frac{\beta x_j}{\sum_i a_{ij}} \tag{5}$$

[STEP 3-3] (Image update) Compute $\vec{x}^{(k+1)}$ by $x_j^{(k+1)} = \max(q_j, \epsilon)$, where $\epsilon > 0$ is a small number to ensure the positivity of pixel value.
[STEP 4] (Convergence check) Increament the iteration number as $k \leftarrow k + 1$ and go to **[STEP 3-1]** until reaching to a stopping criteria.

3.2 Preliminary results

In the current research, we investigate the use of R-MAP and I-MAP methods for solving the interior problem. Here, we discuss the results obtained from a preliminary studies of using R-MAP method. We assume that a single intensity value (μ) inside the ROI is *a priori* known but the positions of pixels having this intensity value are unknown. It is clear that this *a priori* information is easy to be obtained compared to those in the previous work [11–13]. In the previous studies, the interior sub-region should be defined completely (pixel value and pixel position) but in the proposed method, a single intensity value

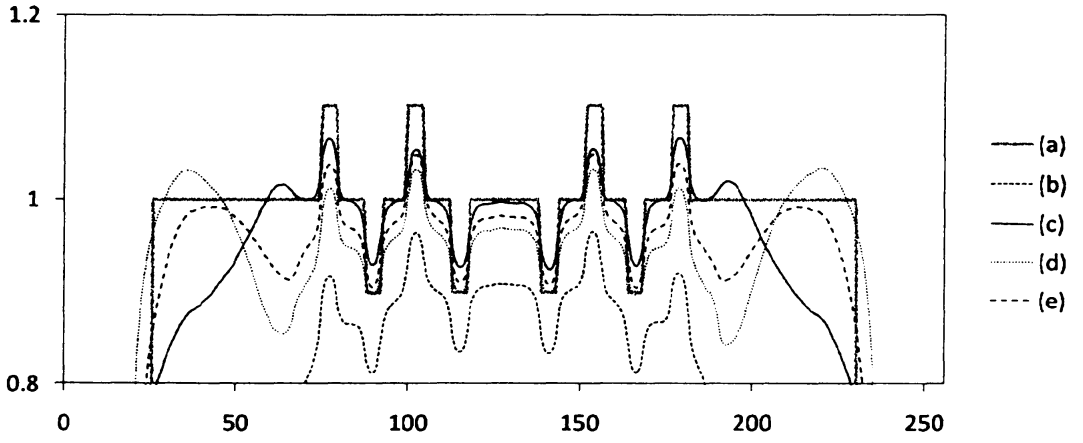

Figure 8: Central profiles corresponding to images in Fig. 7.

(μ) is the only required. We proposed formulating the reference image $\vec{x}^{ref}$ for the R-MAP method such that

$$x_j^{ref} = \begin{cases} \mu & x_j^{ref} \in ROI \\ 0 & (elsewhere) \end{cases} \tag{6}$$

We evaluate the effect of using R-MAP method by a set of simulation studies. In the first simulation we use a uniform disk phantom with hot/cold spots. The image size was 256×256 and the projection data computed with parallel-beam geometry over 256 bins and 256 angles (over 180°) then truncated such that only projection rays passing through the ROI are included. Reconstruction is done using OS-EM and ordered subsets version of R-MAP method with 100 iterations and 4 subsets. In R-MAP method, we assume that the OS is *a priori* known as the region of 120% larger than the exact object. In this study, we use two different values for μ corresponding to a large region (Region A: background region with $\mu = 1.0$) and a small region (Region B: cold spot with $\mu = 0.9$). Reconstructed images are shown in figure 7 and corresponding central profiles are shown in figure 8.

Another simulation study was done using modified FORBILD thorax phantom. We investigate the effect of enforcing a compact OS with OS-EM algorithm and also we evaluate the using R-MAP method with *a priori* known intensity values corresponding to large and small regions (Region A and Region B in figure 9(a)). The image size was 512×512 and the projection data computed with parallel-beam geometry over 512 bins and 512 angles (over 180°). Other simulation setups remains similar to those of the previous study. Reconstructed images are shown in figure 9.

Finally, we evaluate the proposed method using real CT data corresponding to a single slice of head imaging obtained from Toshiba CT scanner. Projection data was measured using the fan-beam geometry with 616 views (over 360°) and 512 detector channels. The projection data was rebinned into parallel-

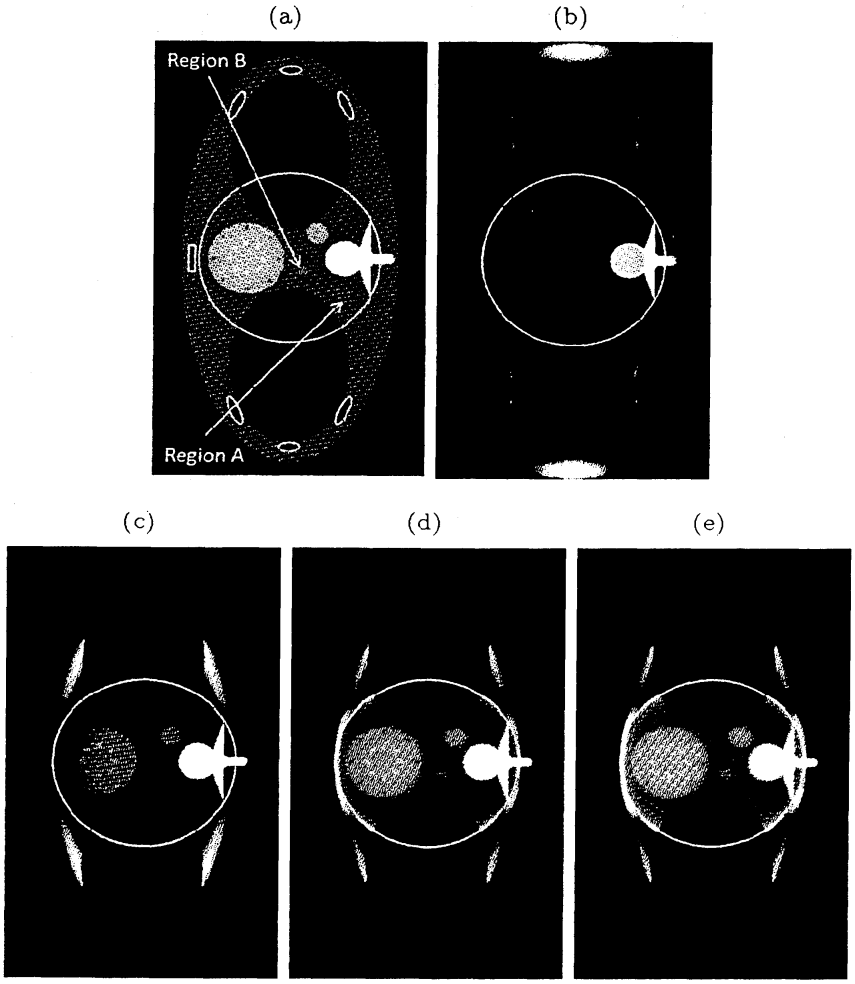

Figure 9: Reconstructed images of the modified FORBILD thorax phantom. (a) Phantom, interior ROI and regions used to computed reference images for R-MAP method, reconstructed images with (b) OS-EM method with unknown OS, (c) OS-EM method with compact OS corresponding to 120% of the exact object, (d) R-MAP method with μ equals the intensity value of region A and (e) R-MAP method with μ equals the intensity value of region B. Gray scale is [0.94 1.1]

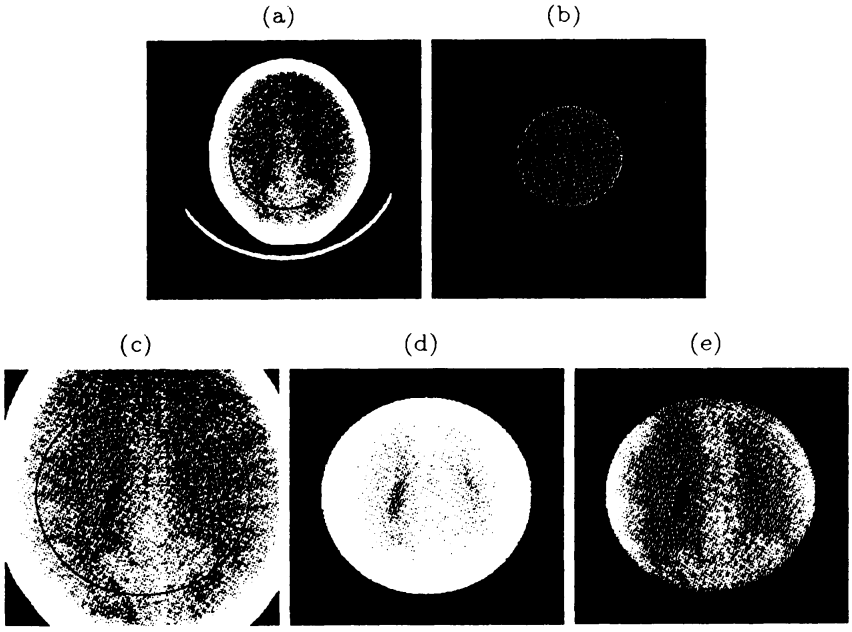

Figure 10: Head CT data. (a) Reconstructed image from full scan data using OS-EM and the interior ROI, (b) reference image for R-MAP method, (c) is magnification of (a), reconstructed ROI by using (c) OS-EM method and (d) R-MAP method. Gray scale is [0.0 0.8].

beam with 300 views (over 180°) and 512 radial bins. Image grid corresponding to the whole image was set to of 512×512 pixels and the ROI was selected as a circular internal region with a radius of 200 pixels. The OS-EM algorithm (200 iterations/16 subsets) was used to reconstruct the whole object using the full scan data as shown in figure 10(a). The value of μ for reference image is computed as the average value of the internal ROI using image reconstructed from full scan data. Then a reconstruction was performed for ROI imaging using the OS-EM and R-MAP methods. Reconstructed ROI images are shown in figure 10.

4 Conclusion

We provide a brief review for the recent development in the interior tomography. It becomes true that exact reconstruction of interior ROI is possible under the assumption that a small subregion is *a priori* known. In clinical application, achieving accurate estimate of this subregion is challenging due to registration errors and other related restrictions. We investigate a new approach to effectively compute the *a priori* information such that we limited the required information to the intensity value only. We currently study implementing the proposed approach on cardiac imaging.

References

[1] F. Natterer, *The Mathematics of Computerized Tomography.* Philadelphia, USA: SIAM, 1986.

[2] R. M. Lewitt, "Processing of incomplete measurement data in computed tomography," *Med. Phys.*, vol. 6, no. 5, pp. 412–417, 1979.

[3] K. Ogawa, M. Nakajima, and S. Yuta, "A reconstruction algorithm from truncated projections," *IEEE Trans. Med. Imag.*, vol. 3, pp. 34–40, Mar. 1984.

[4] A. K. Louis and A. Rieder, "Incomplete data problems in x-ray computerized tomography ii. truncated projections and region-of-interest tomography," *Numer. Math.*, vol. 56, pp. 371–383, 1989.

[5] P. Kuchment, K. Lancaster, and L. Mogilevskaya, "On local tomography," *Inverse Problems*, vol. 11, no. 3, pp. 571–589, 1995.

[6] B. Ohnesorge, T. Flohr, K. Schwarz, J. Heiken, and K. T. Bae, "Efficient correction for ct image artifacts caused by objects extending outside the scan field of view," *Med. Phys.*, vol. 27, pp. 39–46, 2000.

[7] F. Noo, R. Clackdoyle, and J. D. Pack, "A two-step hilbert transform method for 2d image reconstruction," *Phys. Med. Biol.*, vol. 49, no. 17, pp. 3903–3923, 2004.

[8] X. Pan, Y. Zou, and D. Xia, "Image reconstruction in peripheral and central regions-of-interest and data redundancy," *Med. Phys.*, vol. 32, no. 3, pp. 673–684, 2005.

[9] B. Zhang and G. L. Zeng, "Two-dimensional iterative region-of-interest (roi) reconstruction from truncated projection data," *Med. Phys.*, vol. 34, no. 3, pp. 935–944, 2007.

[10] M. Defrise, F. Noo, R. Clackdoyle, and H. Kudo, "Truncated hilbert transform and image reconstruction from limited tomographic data," *Inverse Problems*, vol. 22, no. 3, pp. 1037–1053, 2006.

[11] H. Kudo, M. Courdurier, F. Noo, and M. Defrise, "Tiny *a priori* knowledge solves the interior problem in computed tomography," *Phys. Med. Biol.*, vol. 53, no. 9, pp. 2207–2231, 2008.

[12] M. Courdurier, F. Noo, M. Defrise, and H. Kudo, "Solving the interior problem of computed tomography using a priori knowledge," *Inverse Problems*, vol. 24, no. 6, p. 065001 (27pp), 2008.

[13] Y. Ye, H. Yu, Y. Wei, and W. G., "A general local reconstruction approach based on a truncated hilbert transform," *Int. J. Biomed. Imag.*, vol. 2007, no. 9, p. 63634, 2007.

[14] H. Yu, J. Yang, M. Jiang, and G. Wang, "Interior spect - exact and stable roi reconstruction from uniformly attenuated local projections," *Comm. Numer. Meth. Eng.*, vol. 25, no. 6, pp. 693–710, 2009.

[15] D. L. Donoho, "Compressed sensing," *IEEE Trans. Inf. Theory*, vol. 52, pp. 1289–1306, Apr. 2006.

[16] E. J. Candès, J. Romberg, and T. Tao, "Robust uncertainty principles: exact signal reconstruction from highly incomplete frequency information," *IEEE Trans. Inf. Theory*, vol. 52, pp. 489–509, Feb. 2006.

[17] H. Yu and G. Wang, "Compressed sensing based interior tomography," *Phys. Med. Biol.*, vol. 54, no. 13, p. 4341, 2009.

[18] E. A. Rashed and H. Kudo, "Intensity-based bayesian framework for image reconstruction from sparse projection data," *Med. Imag. Tech.*, vol. 27, pp. 243–251, Sept. 2009.

[19] Y. Mameuda and H. Kudo, "New anatomical-prior-based image reconstruction method for pet/spect," in *Nuclear Science Symposium Conference Record, 2007. NSS '07. IEEE*, vol. 6, pp. 4142–4148, 2007.